

3<sup>RD</sup> EUROPEAN CONFERENCE ON PLASMA DIAGNOSTICS (ECPD2019)  
6–10 MAY 2019  
LISBON, PORTUGAL

## Enhancement of an E parallel B type neutral particle analyzer with high time resolution in the Large Helical Device

Y. Fujiwara,<sup>a,1</sup> S. Kamio,<sup>a</sup> K. Ogawa,<sup>a,b</sup> H. Yamaguchi,<sup>a</sup> R. Seki,<sup>a,b</sup> H. Nuga,<sup>a</sup> T. Nishitani,<sup>a</sup>  
M. Isobe,<sup>a,b</sup> M. Osakabe,<sup>a,b</sup> and the LHD Experiment Group

<sup>a</sup>National Institute for Fusion Science, National Institutes of Natural Science,  
322-6 Oroshi-cho, Toki city, Gifu, 509-5292 Japan

<sup>b</sup>The Graduate University for Advanced Studies (SOKENDAI),  
322-6 Oroshi-cho, Toki city, Gifu, 509-5292 Japan

E-mail: [fujiwara.yutaka@nifs.ac.jp](mailto:fujiwara.yutaka@nifs.ac.jp)

**ABSTRACT:** In order to study fast ion confinement and transport mechanisms both in quiescent plasmas and in the presence of magneto-hydrodynamic (MHD) activity, an electric field parallel to the magnetic field type neutral particle analyzer (E||B-NPA) was installed using Micro-Channel Plates (MCPs) in the Large Helical Device (LHD). The E||B-NPA is an established diagnostic used to measure the energy distribution of charge exchange neutral particles escaping from plasmas corresponding to hydrogen, deuterium, and tritium, respectively. The LHD deuterium experimental campaign started in 2017. To obtain more details of MHD behavior, we improved on time resolution performance of the E||B-NPA using a high-speed Pre-Amplifier and Discriminator (PAD) and Latching Scaler Module (LSM). For the last LHD experimental campaign, the E||B-NPA was installed on nearly the equatorial plane of the vacuum chamber to measure the passing energetic particles generated by tangentially injected neutral beams. As the results of the E||B-NPA commissioning, it is confirmed that the E||B-NPA successfully detected the energetic particles and obtained the energy distributions corresponding to hydrogen. Also, the effect of the neutron to E||B-NPA is estimated using the other neutron diagnostics during the experiments.

**KEYWORDS:** Nuclear instruments and methods for hot plasma diagnostics; Plasma diagnostics - charged-particle spectroscopy

<sup>1</sup>Corresponding author.

---

## Contents

<b>1</b>	<b>Introduction</b>	<b>1</b>
<b>2</b>	<b>Enhanced E  B-NPA system configuration</b>	<b>2</b>
<b>3</b>	<b>Performance evaluations on a test stand</b>	<b>3</b>
<b>4</b>	<b>Experimental results on LHD</b>	<b>4</b>
4.1	Experimental setup	4
4.2	Calibration of the MCPs sensitivity	4
4.3	Effect of radiation	5
<b>5</b>	<b>Conclusion</b>	<b>6</b>

---

## 1 Introduction

A magnetic confinement fusion reactor requires the combustion maintenance of plasma due to energetic particles such as alpha particles produced by the fusion reaction. Therefore, it is important to understand the behavior of energetic particles in the magnetic confinement fusion device. To investigate the behavior of energetic particles which were produced by tangentially injected Negative Neutral Beams (NNB) ( $< 200$  keV), as part of the diagnostic suite for studying energetic particles, a fast-ion charge exchange spectroscopy system was installed on the Large Helical Device (LHD) [1–3]. However, Neutral Particle Analyzers (NPAs) are also desirable for measuring energetic particles directly. NPA can measure the energy spectrum of the energetic particles which are charge exchanged with the neutral particles inside the plasma. Therefore, NPA is used for research on energetic particle confinement and studies on the energy transfer between fast ions and the bulk plasma are advancing. Also, in LHD, many kinds of NPA are adopted for measuring the energetic particles [4, 5], and energetic particle confinement and transfer mechanism studies are advancing [6]. To understand the energetic particle confinement, not only the experiment but also the development of the simulation code is important. From the point of view of the validation of the simulation code [7], the information of the spatial distribution is important. In the study of the instability driven by energetic particles, the time evolution of the energetic particle spectra in various locations should be a key parameter to understand the phenomenon. In order to observe the spatial distribution of the energetic particle's energy spectrum, silicon-diode-based NPA arrays are often used [8].

Furthermore, an electric field parallel to the magnetic field type neutral particle analyzer (E||B-NPA) diagnostic system was investigated by a broad range of ion-related phenomena at the Princeton Plasma Physics Laboratory (PPPL) for neutral particle diagnostics on the Tokamak Fusion Test Reactor (TFTR) in 1998 [9]. This diagnostic system is very large and expensive. The E||B-NPA uses a magnetic field for energy resolution and an electric field for mass resolution. The

E||B-NPA can measure energetic particles from 0.5 to 200 keV/amu. The upper limit depends on the coil power supply and the cooling capacity of the coil. The E||B-NPA can measure particles between Mass/Charge = 1 ~ 3. This is an important capability in mixed gas experiments. The LHD experimental campaign started the deuterium experimental campaigns in 2017. Therefore, the E||B-NPA is able to measure the complex data in this experimental campaign by using the device's capabilities. However, the electrical circuit design of the E||B-NPA is outdated. In this study, we focus on improving the design of E||B-NPA which would lead to higher time resolution to measure fast phenomenon. As a result, the E||B-NPA became a very useful tool for obtaining more details of not only typical MHD behavior but also of intermittent MHD behavior that appeared suddenly and for a short time.

## 2 Enhanced E||B-NPA system configuration

The basic measurement concept does not change. The E||B-NPA installed Micro-Channel Plates (MCPs) as detectors. In this work, the electrical circuit of E||B-NPA was modified to improve the time resolution. Figure 1 shows schematic circuit diagrams of the E||B-NPA system. Figure 1(a) and figure 1(b) shows before and after the modifications, respectively. The previous circuit design of the E||B-NPA had three arrays for mass/charge resolution, with each array containing 39 channels for the energy resolution. Since the analog signal from the MCPs is weak, ideally a short length cable would be used from the MCPs to the Pre-Amplifier and Discriminators (PADs). From there, the PADs would be converted to a digital signal. However, the system was not able to use a short length cable due to limited space next to the E||B-NPA and the size of the PADs circuit. Thus, the previous system used the buffer amplifier to transmit the weak analog signal from MCPs to the PADs through a 3 m cable. On the previous circuit system, the ability of processing was under 5 MHz as a scaler, because the pulse width of the output signal from PADs was about 200 ns.

The new E||B-NPA system installed a discriminator with a high Integrated Circuit (IC). The size of the PADs were significantly reduced, thus it is possible to set PADs near the feedthrough and use the short cable of 0.3 m between the feedthrough and the PAD. For that reason, the buffer amplifier was no longer needed. The high-speed PADs are made by Techno-AP, and the name of the product is APG1916. The latching scaler modules (LSMs) are made by Techno-AP, and the name of the product is APV2716L. The maximum count is 16 bits. The ability of processing expects under 100 MHz as a scaler, the time resolution of E||B-NPA measurement becomes up to 10  $\mu$ s. On the new system, the E||B-NPA has three arrays for mass/charge resolution, with each array containing 32 channels for the energy resolution.

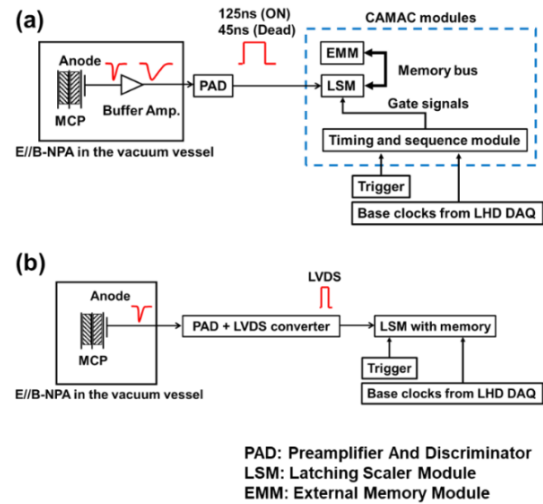


**Figure 1.** Schematic circuit diagrams of the E||B-NPA system. (a) shows before the modification and (b) shows after the modification.

Through these modifications, the E||B-NPA is also able to achieve a vacuum much faster than the previous system, reducing the pump-down time from 2 months to just 2 weeks. The new system is also more energy-efficient, thereby reducing costs. On the new system, to save power, the analog signal is converted to a digital Low Voltage Differential Signal (LVDS) at the converter. We changed cables between the PADs and LSMs. The previous cable was expensive due to using the triplex cable with 3 pin LEMO connector. On the other hand, the new cable has good cost performance because of using the Ethernet cable (category 5e) with RJ45 connector. Then, the one Ethernet cable can transmit the signals of the four channels.

Figure 2 shows the photograph of the enhanced E||B-NPA system configurations. Figure 2(a) is the photograph of the detector. Figure 2(b) is the photograph of the PADs and the LVDS converters. As shown in figure 2(a), we removed buffer amplifiers and changed all wires of the MCP circuit from polyvinyl chloride wires to semi-rigid coaxial wires. The semi-rigid coaxial wire reduces electrical noise, making it possible to transmit weak analog voltage signals without buffer amplifiers. As shown in figure 2(b), the high-speed PAD consists of 6 circuits, with each circuit connected to 4 Ethernet cables. The Ethernet cables can transmit the LVDS signal up to 100 m.

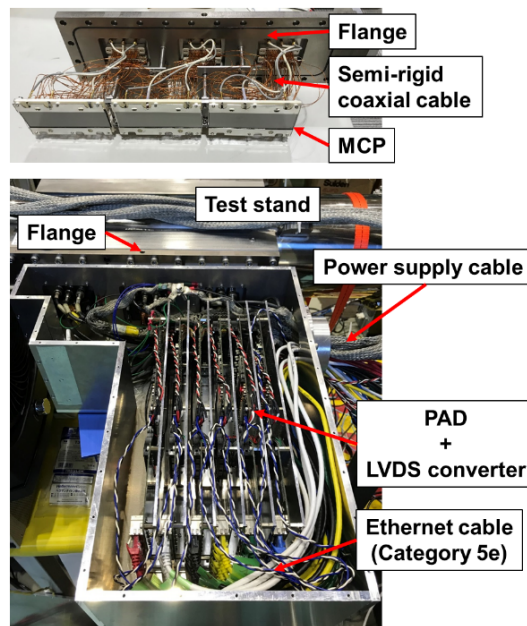


**Figure 2.** The photograph of the enhanced E||B-NPA system configurations. Figure 2(a) is the photograph of the detector. Figure 2(b) is the photograph of the PADs and the LVDS converters.

### 3 Performance evaluations on a test stand

A method using charged particle beams is used to evaluate the operation of E||B-NPA on charged particles [9]. However, this method requires a large-scale device. At this time, in order to evaluate the performance of the enhanced E||B-NPA system,  $^{241}\text{Am}$  was used as an electrically charged particle source.  $^{241}\text{Am}$  is known as a mono-energetic alpha particle source. Using  $^{241}\text{Am}$  made it possible to easily evaluate charged particles of NPA. Figure 3 shows the typical pulse shape of the detected signal. The pulse length of the signal is approximately 5 ns, and the amplitude of the signal is approximately 500 mV. Therefore, the total counts should be less than 200 Mcps to avoid the signal pile-up. The threshold level should be

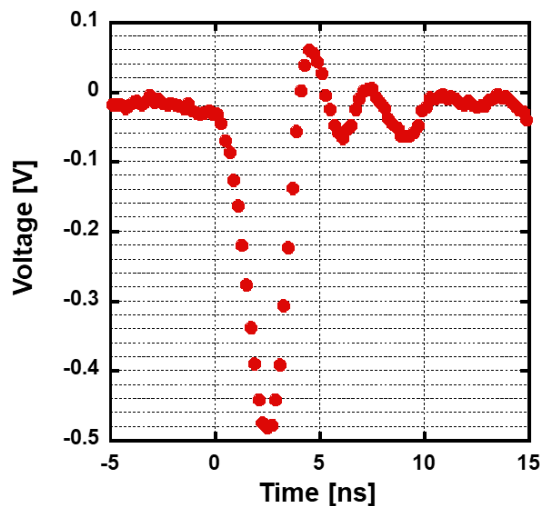


**Figure 3.** The typical detected pulse shape of the  $^{241}\text{Am}$  alpha source on the test stand.

around 200 mV in consideration of the noise level. The ability of processing was confirmed under 100 MHz as a scaler because the pulse width of the output signal from the PAD of the new E||B-NPA system was approximately 5 ns.

## 4 Experimental results on LHD

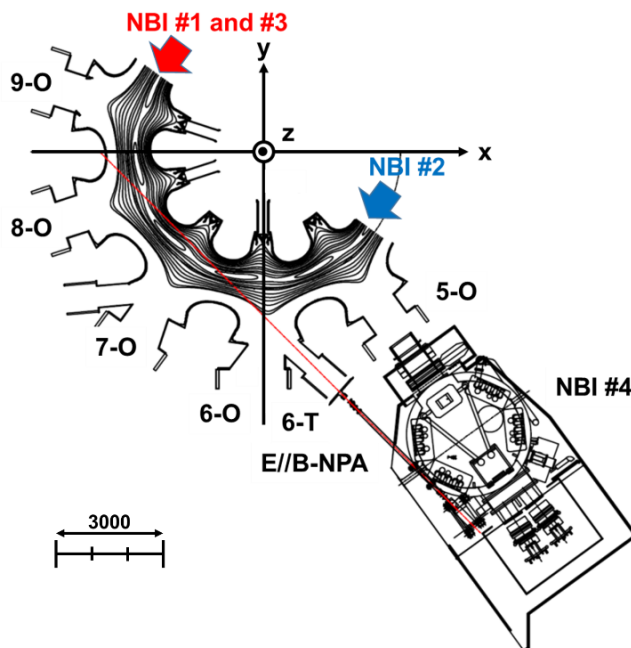
### 4.1 Experimental setup

Figure 4 shows the schematic toroidal cross-section view of LHD and the geometrical arrangement of the E||B-NPA. The MCPs are located at  $x = 5505$  mm,  $y = -10188$  mm, and  $z = -110$  mm from the center of LHD. The E||B-NPA was installed at the 6-T port of LHD and it is possible to measure passing energetic particles tangentially injected from the Neutral Beam Injection (NBI) #1 and #3. The distance between the 6-T port and the MCPs is 4693 mm. In figure 5, the distributions of pitch angles along E||B-NPA sight line is shown as a function of normalized minor radius. The pitch angle and normalized minor radius ( $r/a$ ) distributions along the LOS of E||B-NPA for the LHD standard magnetic field configuration ( $R_{ax} = 3.6$  m). The LSMs and control computer are installed in the basement to avoid the high neutron flux, and the LSMs and PADs are connected by using 50 m Ethernet cables. The electrical circuit system was installed in a metal box to reduce noise, as shown in figure 2(b). To dissipate the heat generated inside the box by discriminators, the box was installed one fan on the top and two fans on the side. The entire E||B-NPA, the electrical circuits, and the control system were covered with 10 cm polyethylene plates and 5 mm boron sheets to reduce the radiation effect.

Figure 6 shows the typical detected pulse shape of the energetic charged particle on LHD. The signal intensity measured in the LHD experiment was about one-tenth of the signal of the experiment using  $^{241}\text{Am}$  on the test stand. The difference between figure 3 and figure 6 is the existence of electric and magnetic fields. The presence of a magnetic field is known to decrease the electrical signal intensity of the electron-multiplying system.

### 4.2 Calibration of the MCPs sensitivity

Figure 7 shows (a) the typical counting rate for each energy channel on H array before the calibration, (b) the relative calibration factor for each energy channel, and (c) the typical counting rate for each energy channel on H array after the calibration. We used data from SN #153042 to SN #153081 on



**Figure 4.** The schematic toroidal cross-section view of LHD and the geometrical arrangement of the E||B-NPA.

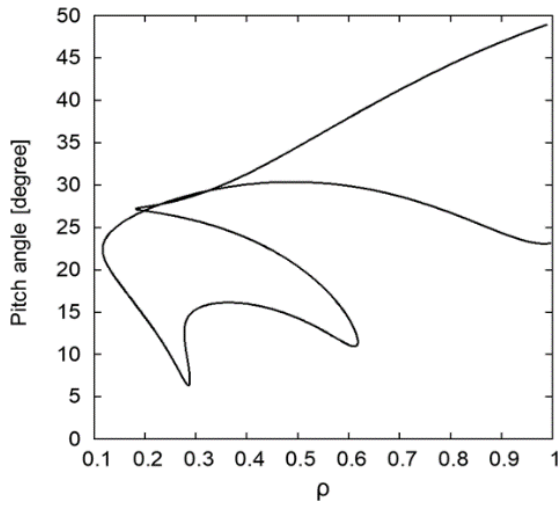


**Figure 5.** The distributions of pitch angles along E||B-NPA sight line on LHD.

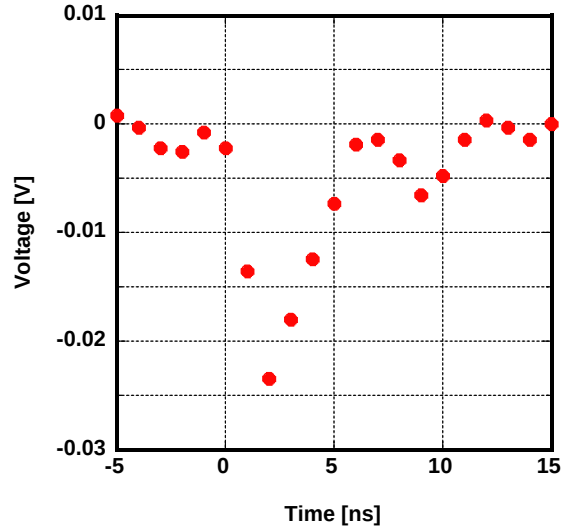


**Figure 6.** The typical detected pulse shape of the energetic charged particle on LHD.

LHD experiments for calibration (4.3 s ~ 4.4 s). Measurement data was acquired by changing the magnetic field strength of E||B-NPA from 0.8 kG to 3.0 kG. All data at (4.3 s ~ 4.4 s) are almost the same experimental conditions of LHD. In this experiment, the location of the magnetic axis position in the vacuum field is 3.6 m and the magnetic field strength of the discharge is 2.75 T in the opposite field direction of the LHD standard configurations. The plasma was the pure hydrogen discharge. The experiment was performed by the injected the NBI #1 ~ 185 keV, the NBI #2 ~ 152 keV, the NBI #3 ~ 161 keV, NBI #4 ~ 45 keV, and NBI #5 ~ 45 keV. In this observation geometry, the E||B-NPA can observe co-passing particles (produced by the NBI #1 and NBI #3). Therefore, all data points are expected to be on the same line. However, as shown in figure 7(a), all data are not on the same line because MCPs sensitivity are different for each channel. Thus, calibration values for each channel of MCPs were obtained by assuming that the counting rate at the same energy should be equal at all magnetic field strength points in figure 7(a). Thus, figure 7(b) is the obtained relative calibration factor for each energy channel. Then, we can estimate the relative counting rate for each channel, as shown in figure 7(c). The figure 7(c) is consistent with expected experiment results because all curves lie on each other and slowing down passing EPs from NBI #1 and NBI #3 are detected.

### 4.3 Effect of radiation

It is known that radiation affect semiconductor devices [10–12]. In order to study the radiation effect in the MCPs, experiments using typical tangential NBI-heated discharges, which produce neutrons, were used. As already mentioned, the entire E||B-NPA system was covered with polyethylene plates and boron sheets by which energetic neutrons become thermal neutrons. The stainless steel gate valve to the E||B-NPA was closed, blocking the neutral particles but allowing neutrons and gamma rays to pass through. Figure 8 shows the time evolutions of (a) the neutron emission rate measured by a Fission Chamber (FC) [13] and (b) the counting rate measured by E||B-NPA while the gate valve is closed. Figure 8(c) shows the radiation effect on the MCPs. We used data from SN #148506

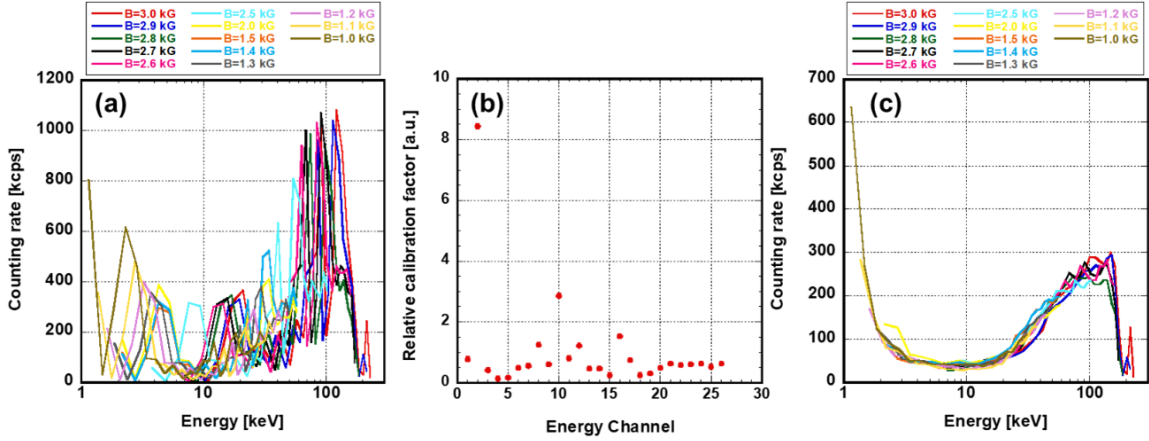


**Figure 7.** (a) the typical counting rate for each energy channel on H array before the calibration, (b) the relative calibration factor for each energy channel, and (c) the typical counting rate for each energy channel on H array after the calibration.

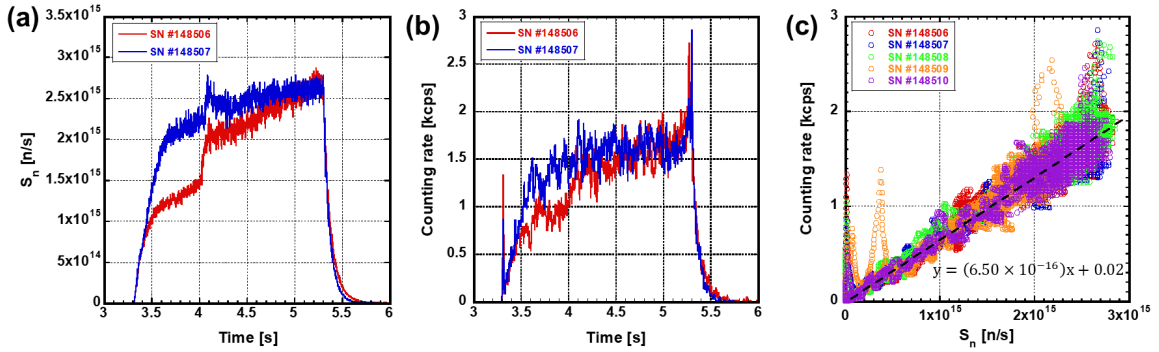


**Figure 8.** Time evolutions of (a) the neutron emission rate measured by FC and (b) the typical counting rate measured by E||B-NPA while the gate valve is closed. (c) The radiation effect for the E||B-NPA.

to SN #148510 on LHD experiments for studying the radiation effect in the MCPs (3.0 s ~ 6.0 s). It was confirmed that every channel of MCPs were similarly affected by the radiation. The neutron signal level scales linearly with the amount of neutron emission. Therefore, the radiation effect can be estimated using other neutron diagnostics during experiments. As shown in figure 8(c), the radiation effect on MCPs is considered to be less than 3 kcps because the neutron emission rate in LHD is up to  $3.3 \times 10^{15}$  n/s [14]. From figure 8(c), the linear relationship between the neutron emission rate and the average radiation effect of MCPs can be expressed by the following formula ( $y = (6.50 \times 10^{-16})x + 0.02$ ;  $y$  is average counting rate (unit is kcps) by radiation effect,  $x$  is the neutron emission rate measured by FC). From the formula, the average measurement error bar by radiation effect can be estimated in the E||B-NPA on LHD.

## 5 Conclusion

The E||B-NPA was newly enhanced using high time resolution system in LHD hydrogen and deuterium experiments. The E||B-NPA was installed on nearly the equatorial plane of the vacuum

chamber to measure the passing energetic particles generated by tangentially injected neutral beams. By the modification, the ability to process the signal became under 100 MHz as a scaler, because the pulse width of signal from MCP to PAD of the enhanced E||B-NPA system was approximately 5 ns. The relative calibration factor was obtained for each channel used in the LHD experimental campaign. Also, the radiation effect on E||B-NPA was evaluated quantitatively. In order to confirm the radiation effect in MCP, the gate of E||B-NPA was closed. The radiation effect on MCPs is considered to be less than 3 kcps because the neutron emission rate in LHD is up to  $3.3 \times 10^{15}$  n/s. The linear relationship between the neutron emission rate and the average radiation effect of MCPs can be expressed by the following formula ( $y = (6.50 \times 10^{-16})x + 0.02$ ;  $y$  is average counting rate (unit is kcps) by radiation effect,  $x$  is the neutron emission rate measured by FC). The average measurement error bar by radiation effect can be estimated by using the formula in the E||B-NPA on LHD.

## Acknowledgments

This work was supported by the LHD project budget (ULRR006, ULRR035, ULRR036, and ULRR702).

## References

- [1] M. Osakabe et al., *Fast ion charge exchange spectroscopy measurement using a radially injected neutral beam on the large helical device*, *Rev. Sci. Instrum.* **79** (2008) 10E519.
- [2] T. Ito et al., *Effect of Halo Neutrals on Fast-Ion Charge Exchange Spectroscopy Measurements in LHD*, *Plasma Fusion Res.* **5** (2010) S2099.
- [3] Y. Fujiwara et al., *Evaluation of an energetic particle profile using a tangential-FIDA diagnostic in the Large Helical Device*, *Plasma Fusion Res.* **14** (2019) 3402129.
- [4] M. Isobe et al., *Fast-Particle Diagnostics on LHD*, *Fusion Sci. Tech.* **58** (2010) 426.
- [5] M. Osakabe et al., *Experimental observations of enhanced radial transport of energetic particles with Alfvén eigenmode on the LHD*, *Nucl. Fusion* **46** (2006) S911.
- [6] M. Osakabe et al., *Fast-Ion Confinement Studies on LHD*, *Fusion Sci. Tech.* **58** (2010) 131.
- [7] S. Äkäslompolo et al., *Validating the ASCOT modelling of NBI fast ions in wendelstein 7-X stellarator*, 2019 *JINST* **14** C10012.
- [8] M. Osakabe et al., *Development and energy calibration of Si-FNA for LHD fast ion measurement*, *Rev. Sci. Instrum.* **72** (2001) 788.
- [9] S.S. Medley and A.L. Roquemore, *Construction and operation of parallel electric and magnetic field spectrometers for mass/energy resolved multi-ion charge exchange diagnostics on the Tokamak Fusion Test Reactor*, *Rev. Sci. Instrum.* **69** (1998) 2651.
- [10] T. Nishitani et al., *Japanese contribution to ITER task of irradiation tests on diagnostics components*, *Fusion Eng. Des.* **42** (1998) 443.
- [11] S. Yamamoto et al., *Impact of irradiation effects on design solutions for ITER diagnostics*, *J. Nucl. Mater.* **283–287** (2000) 60.

- [12] K. Ogawa et al., *Investigation of irradiation effects on highly integrated leading-edge electronic components of diagnostics and control systems for LHD deuterium operation*, *Nucl. Fusion* **57** (2017) 086012.
- [13] M. Isobe et al., *Wide dynamic range neutron flux monitor having fast time response for the Large Helical Device*, *Rev. Sci. Instrum.* **85** (2014) 11E114.
- [14] M. Isobe et al., *Fusion neutron production with deuterium neutral beam injection and enhancement of energetic-particle physics study in the large helical device*, *Nucl. Fusion* **58** (2018) 082004.